Isotropic–liquid crystal phase equilibrium in semiflexible polymer solutions: xanthan, a rigid polyelectrolyte*

Takahiro Sato†, Takashi Kakihara and Akio Teramoto
Department of Macromolecular Science, Osaka University, Toyonaka, Osaka 560, Japan
(*Received 4 December 1989; accepted 21 December 1989*)

The isotropic–liquid crystal phase equilibrium was investigated for aqueous sodium chloride (NaCl) solutions of an ionic double-helical polysaccharide, xanthan. The phase boundary concentrations between isotropic and biphasic regions and between biphasic and cholesteric regions were very low at small NaCl concentration C_s but increased sigmoidally with increasing C_s to approach those for the corresponding neutral polymers. The phase boundary concentrations were reproduced fairly accurately by the Onsager theory modified by Odijk to worm-like polyelectrolyte solutions with a Philip–Wooding electrostatic potential for charged cylinders.

(Keywords: liquid crystal; phase equilibrium; polyelectrolyte; xanthan; electrostatic interaction)

INTRODUCTION

Xanthan is an ionic polysaccharide produced by a plant pathogen. Previous dilute-solution studies[1–6] revealed that xanthan dissolves in aqueous salt as a rigid double-stranded helix. Thus, this polysaccharide can be regarded as an example of a rigid polyelectrolyte.

Rinaudo *et al.*[7] found that an aqueous solution of xanthan forms a cholesteric mesophase above a polymer concentration as low as 3.5 wt%. Such a low critical concentration is characteristic of lyotropic liquid crystals of rigid polyelectrolytes. For example, the aqueous solution of tobacco mosaic virus (TMV) has a very low critical concentration[8,9]. Onsager[10] showed that the electrostatic repulsive interaction is responsible for the low critical concentration of TMV.

As pointed out by Odijk[11] in his review, the isotropic–liquid crystal phase behaviour for such a charged polymer system, especially its ionic strength dependence, has not been studied in detail. In this paper, we present the isotropic–liquid crystal phase boundary concentration for aqueous xanthan as a function of added salt (NaCl) concentration. Further, the experimental data obtained are compared with Onsager's theory[10] modified by Odijk[11] for semiflexible polyelectrolytes. At the completion of the present study, we noticed a recent paper by Fraden *et al.*[12], who found a similar charge effect on the phase diagram for TMV in phosphate buffer.

EXPERIMENTAL

Following the procedure established before[3], a commercial xanthan sample (Kelco's Keltrol) was sonicated, purified and repeatedly fractionated by fractional precipitation. An appropriate middle fraction was chosen and was further divided into two parts using isotropic–liquid crystal phase separation[13]. The sample recovered from the liquid-crystal phase was converted to Na salt form and used for phase separation experiments. Its molecular weight was estimated to be 6.14×10^5 using the established viscosity–molecular weight relation[5].

The isotropic–liquid crystal phase separation experiment was done at 25°C and at added NaCl molar concentration C_s ranging from 0.005 to 1 M by the procedure employed before[14]; a biphasic solution of xanthan was prepared in a calibrated stoppered tube, kept standing for 1 day at 25°C, and centrifuged at 4000 rpm at 25°C to attain complete phase separation. The volume of each separated phase was determined from its column height. The polymer mass concentration c of the solution was calculated from:

$$c = w/[(1-w)v_0 + wv_p]$$

with w being the polymer weight fraction and v_0 the solvent specific volume; the partial specific volume v_p of the polymer was taken to be $0.571\,\mathrm{cm^3\,g^{-1}}$ irrespective of C_s.

RESULTS

Figure 1 shows the relation between the average polymer concentration c and the relative volume Φ of the isotropic phase in biphasic mixtures of xanthan with different C_s. The data points for each C_s almost follow a straight line. The extrapolations of this line to $\Phi = 1$ and 0 give the phase boundary concentrations c_i between isotropic and biphasic regions and c_a between liquid-crystal and biphasic regions, respectively.

Figure 2 depicts the C_s dependence of c_i and c_a obtained. At low C_s, both c_i and c_a are very low, indicating that aqueous xanthan forms a cholesteric mesophase at low polymer concentrations. As C_s increases, c_i and c_a increase sigmoidally, approaching higher values comparable to those for neutral rigid polymer solutions (e.g. schizophyllan[15] and polypeptide[16] solutions). This strong C_s dependence of the phase boundary concentration demonstrates the importance of the electrostatic potential

---

* Dedicated to Professor Walther Burchard on the occasion of his 60th birthday

† To whom correspondence should be addressed

0032-3861/90/050824-05

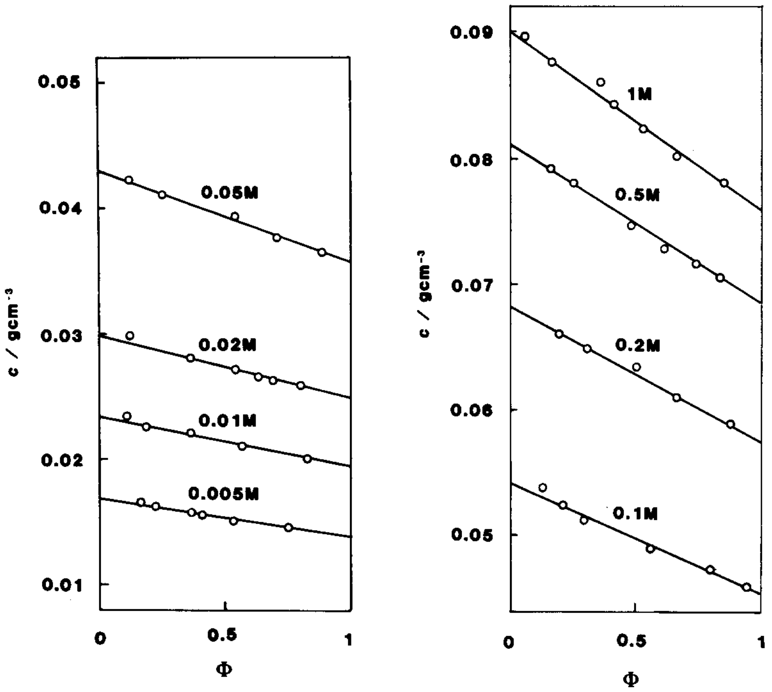

Figure 1 Plots of the average polymer concentration c vs. the volume fraction Φ of the isotropic phase for different C_s at 25°C

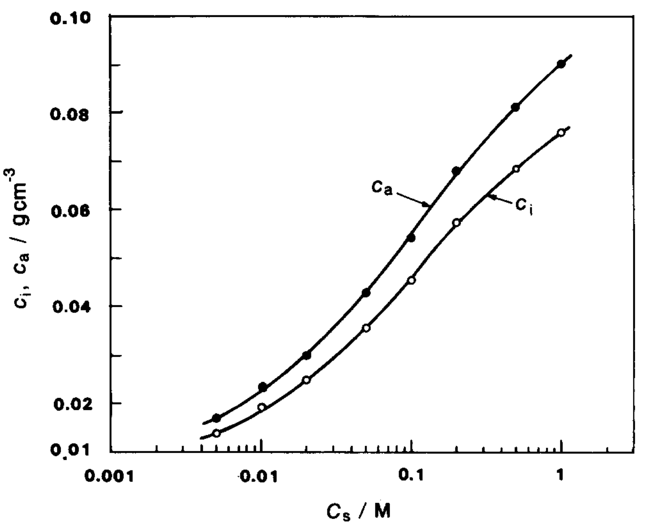

Figure 2 Salt concentration dependences of the phase boundary concentrations c_i and c_a for aqueous xanthan at 25°C

for the isotropic–liquid crystal phase equilibrium in aqueous xanthan. The recent data of Fraden *et al.*[12] for TMV in phosphate buffer showed a similar dependence.

DISCUSSION

Onsager[10] presented a theory for the isotropic–liquid crystal phase equilibrium in a rod-like polyelectrolyte solution. Assuming the phase boundary concentrations c_i and c_a to be very low, he used the second virial approximation to formulate the Helmholtz free energy ΔF of the solution:

$$\Delta F/nk_BT=\mu_0/k_BT-1+\ln c'+\sigma+B_2c' \qquad (1)$$

where n is the number of rod-like molecules, k_B the Boltzmann constant, T the absolute temperature, μ_0 the standard chemical potential of the solute, c' the number density of rod-like molecules, σ the orientational entropy loss upon formation of the liquid-crystal phase, and B_2 the second virial coefficient.

Odijk[11] extended the Onsager theory to worm-like polyelectrolytes, following Khokhlov and Semenov's procedure[17], which was originally applied to neutral semiflexible polymers. That is, he replaced σ in equation (1) by σ_{KS}, which contains a conformational entropy loss as well as the orientational entropy loss of worm-like chains due to the formation of liquid crystal. With the Onsager trial function for the orientational distribution function $f(\Omega)$ of the tangent vector of the worm-like chain, σ_{KS} is given by:

$$\sigma_{KS}=\begin{cases}(\alpha-1)N/2+\ln(\alpha/4) & (\alpha N\gg 1) \qquad (2a)\\ \ln\alpha-1+(\alpha-1)N/3 & (\alpha N\ll 1) \qquad (2b)\end{cases}$$

where N is the number of Kuhn's statistical segments per molecule and α is the orientational parameter contained in the Onsager trial function.

Further, Odijk proposed to approximate B_2 for worm-like polyelectrolytes by that for rod-like polyelectrolytes, which is given by:

$$B_2=-\tfrac{1}{2}\int\int[\beta_c(\gamma)+\beta_{el}(\gamma)]f(\Omega)f(\Omega')\,d\Omega\,d\Omega' \qquad (3)$$

Here, $\beta_c(\gamma)$ and $\beta_{el}(\gamma)$ are the irreducible cluster integrals for the hard core and the electrostatic potential of the charged rod, respectively; γ represents the angle between two rods oriented at Ω and Ω'. For a rod with length L and hard-core diameter d:

$$\beta_c(\gamma)=-2L^2d|\sin\gamma| \qquad (4)$$

and

$$\beta_{el}(\gamma)=2L^2d|\sin\gamma|\int_d^\infty[\exp(-w_{el}/k_BT)-1]\,dx \qquad (5)$$

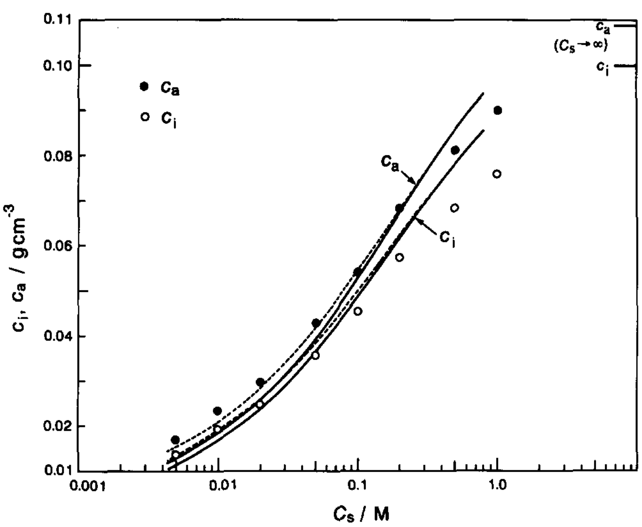

Figure 3 Comparison of the experimental data (circles) with the modified Onsager theory (curves) for worm-like polyelectrolytes: full curves, calculated with κ at infinite dilution (equation (7)); broken curves, calculated with the effective κ at finite polymer concentration (see 'Appendix')

where w_{el} is the electrostatic interaction between two rods and x is the shortest distance between the centre lines of the two rods. Because w_{el} appears in the Mayer f function, the exact functional form of w_{el} at small x is not needed, because there the f function takes a value very close to -1. Thus, as proposed by Stroobants *et al.*[18], Philip and Wooding's solution[19] of the Poisson–Boltzmann equation for the charged cylinder can provide a relevant expression for w_{el}:*

$$w_{el}/k_BT = A \exp(-\kappa x)/|\sin\gamma| \tag{6}$$

Here, κ is the reciprocal of the Debye screening length and A is a function of $\kappa d/2$, which is defined in Philip and Wooding's paper[19]. At infinite dilution of polymer, κ can be calculated from:

$$\kappa^2 = 8\pi Q n_s \tag{7}$$

where Q is the Bjerrum length and n_s is the number density of added salt (1–1 electrolyte). To a first approximation, this equation may be used to calculate w_{el} at finite polymer concentrations (for a refinement of this approximation, see the 'Concluding Remarks' and 'Appendix').

We calculated the isotropic–liquid crystal phase boundary concentrations c_i and c_a from the phase coexistence equations and the stabilization condition of the anisotropic phase, which were all derived from ΔF given in equation (1) with σ replaced by σ_{KS}. The free energy ΔF contains four molecular parameters, i.e. L, N, d and the linear charge density ν of the polymer. The values of L and N for our sample were 316.5 nm and 1.32, which were estimated from its molecular weight M with the molecular weight M_L per unit contour length and the persistence length q of xanthan taken to be 1940 cm^{-1} and 120 nm, respectively[5]; $L = M/M_L$, $N = L/2q$. It should be noted that q of xanthan is insensitive to C_s at 0.005–1.0 M (ref. 20). The values of d and ν were taken to be 2.2 nm and 3.0 nm^{-1}, respectively, from the molecular model of xanthan double helix[21] with degree of pyruvation of 0.4. As in the previous paper[22], the values of c_i and c_a at $N = 1.32$ were evaluated by interpolating c_i and c_a calculated for $N = 0$ (using equation (2b)) and $N \geqslant 1.5$ (equation (2a)) at fixed L.

Figure 3 compares the theoretical curves (full curves) for c_i and c_a calculated as above† with our experimental data indicated by circles. Here, we note that the theoretical curves have been constructed with no adjustable parameters. The experimental sigmoidal increases of c_i and c_a with increasing C_s are successfully reproduced by the theory, and the agreement between theory and experiment is almost quantitative.

CONCLUDING REMARKS

We have shown that the Onsager theory[10] modified by Odijk[11] for semiflexible polyelectrolytes agrees fairly well with our experimental data on aqueous xanthan when the Philip–Wooding (PW) electrostatic potential[19] is used. As mentioned before, the modified Onsager theory is based on the second virial approximation. Thus, the above agreement demonstrates that the isotropic–liquid crystal phase behaviour in semiflexible polyelectrolyte solutions can be described fairly accurately by considering up to the second virial term in the free energy. The same conclusion was obtained[14] for solutions of neutral polymers of moderate stiffness $q \gtrsim 30$ nm, and confirmed theoretically by comparison of the Khokhlov–Semenov theory[17] with the second virial approximation and the scaled particle theory containing all virial terms[22]. (Fraden *et al.*[12] favoured a scaled theory due to Lee[23] rather than the Onsager theory to interpret their TMV data. However, we notice that the axial ratio of the TMV is as small as 15, which may be beyond the range in which the Onsager theory can be used[11].)

Recently, Nicolai and Mandel[24] reported that their experimental data of the second virial coefficient for a short DNA sample in aqueous NaCl compared more favourably with the Debye–Hückel–Manning (DHM) potential[25] considering ion condensation than with the PW potential[19] (equation (6)). However, the use of the DHM potential instead of the PW potential gives considerably higher c_i and c_a than our experimental data at higher C_s, and thus Nicolai and Mandel's results seem to be inconsistent with ours.

Both calculations of the second virial coefficient and the phase boundary concentration need the expression of the screening length κ^{-1}. For the former, equation (7) (κ at infinite dilution) is available, while for the latter, it is just approximate because the polymer concentrations c_i and c_a are not necessarily low and are different from each other. Therefore we estimated the finite concentration effect on κ and recalculated c_i and c_a by the method given in the Appendix. The broken curves in *Figure 3* represent c_i and c_a calculated from the modified

---

* Originally, Onsager used a solution of the Poisson–Boltzmann equation for two parallel charged plates to estimate w_{el} for two charged cylinders, and further neglected the γ dependence of w_{el} on orientational averaging in equation (3) for the anisotropic phase. The latter approximation was removed by Stroobants *et al.*[18], whom we followed to calculate B_2 in the anisotropic phase

† The integration in equation (5) can be done analytically only on condition that $A\exp(-\kappa d) > 2$. This condition corresponds to $C_s < 0.8$ M, so that the values of c_i and c_a were not calculated for $C_s > 0.8$ M except for infinite C_s, where the phase boundary concentrations can be calculated from Khokhlov and Semenov's theory[17] for neutral polymers (cf. the horizontal bars on the right side of *Figure 3*)

Onsager theory with the effective screening length. It can be seen that these curves do not deviate appreciably from the corresponding full curves, which reveals that the use of κ at infinite dilution is a good approximation in the calculation of c_i and c_a. At present, we cannot reconcile the inconsistency between our phase diagram data and Nicolai and Mandel's second virial coefficient data. In order to elucidate which potential is relevant, the second virial coefficient in addition to the phase boundary concentrations should be measured for aqueous solutions of xanthan as a function of C_s.

ACKNOWLEDGEMENTS

We would like to thank Professor T. Norisuye for valuable discussion and comment. This work was financially supported by a Grant-in-Aid for Scientific Research, 01470108, from the Ministry of Education, Science and Culture of Japan.

REFERENCES

1 Holtzwarth, G. *Carbohydr. Res.* 1978, **66**, 173
2 Paradossi, G. and Brant, D. A. *Macromolecules* 1982, **15**, 874
3 Sato, T., Norisuye, T. and Fujita, H. *Polym. J.* 1984, **16**, 341
4 Sato, T., Kojima, S., Norisuye, T. and Fujita, H. *Polym. J.* 1984, **16**, 423
5 Sato, T., Norisuye, T. and Fujita, H. *Macromolecules* 1984, **17**, 2696
6 Coviello, T., Kajiwara, K., Burchard, W., Dentini, M. and Crescenzi, V. *Macromolecules* 1986, **19**, 2826
7 Maret, G., Milas, M. and Rinaudo, M. *Polym. Bull.* 1981, **4**, 291
8 Bawden, F. C. and Pirie, N. W. *Proc. R. Soc. Lond. (B)* 1937, **123**, 274
9 Oster, G. J. *J. Gen. Physiol.* 1950, **33**, 445
10 Onsager, L. *Ann. NY Acad. Sci.* 1949, **51**, 627
11 Odijk, T. *Macromolecules* 1986, **19**, 2313
12 Fraden, S., Maret, G., Caspar, D. L. D. and Meyer, R. B. *Phys. Rev. Lett.* 1989, **63**, 2068
13 Itou, T. and Teramoto, A. *Polym. J.* 1984, **16**, 779
14 Itou, T. and Teramoto, A. *Macromolecules* 1988, **21**, 2225
15 Itou, T., Van, K. and Teramoto, A. *J. Appl. Polym. Sci., Appl. Polym. Symp.* 1985, **41**, 35
16 Itou, T., Funada, S., Shibuya, F. and Teramoto, A. *Kobunshi Ronbunshu* 1986, **43**, 191
17 Khokhlov, A. R. and Semenov, A. N. *Physica (A)* 1982, **112**, 605
18 Stroobants, A., Lekkerkerker, H. N. W. and Odijk, T. *Macromolecules* 1986, **19**, 2232
19 Philip, J. R. and Wooding, R. A. *J. Chem. Phys.* 1970, **52**, 953
20 Sho, T., Sato, T. and Norisuye, T. *Biophys. Chem.* 1986, **25**, 307
21 Okuyama, K., Arnott, S., Moorhouse, R., Walkinshow, M. D., Atkins, E. D. T. and Wolf-Ullish, in 'Fiber Diffraction Methods', (Eds. A. D. French and K. H. Gardner), ACS Symp. Ser. No. 141, p. 411, American Chemical Society, Washington, DC, 1980
22 Sato, T. and Teramoto, A. *Mol. Cryst. Liq. Cryst.* in press
23 Lee, S.-D. *J. Chem. Phys.* 1987, **87**, 4972
24 Nicolai, T. and Mandel, M. *Macromolecules* 1989, **22**, 438
25 Manning, G. S. *J. Chem. Phys.* 1969, **51**, 924

APPENDIX

To calculate the electrostatic interaction w_{el} between two polyelectrolyte molecules, the reciprocal of the Debye screening length κ must be given. In the text, we used equation (7), neglecting a finite polymer concentration effect on κ. This appendix presents a method of estimating κ in a solution with a finite polymer concentration and of calculating c_i and c_a with that κ. In what follows, we consider an aqueous solution that contains a 1–1 electrolyte and a polyelectrolyte with z_p univalent negative charges per molecule and counter-ions the same as the cation from the 1–1 electrolyte.

At a finite polymer concentration, the ionic atmosphere about a test polyion should be different from that at infinite dilution, because the mobile ion distribution is affected by the presence of the other polyions. From the following consideration, it turns out that the polyions exclude mobile ions from their vicinity. That is, at the Donnan equilibrium, mobile ions are excluded from the polyelectrolyte solution side and the salt concentration difference between the solvent and the solution sides reaches Γn_e at equilibrium. Here, Γ is the Donnan salt exclusion coefficient and n_e is the number density of charges on the polymers (i.e. $n_e = z_p c'$). Thus, to equilibrate the polyelectrolyte solution with the salt concentration n_s, the solvent side must possess a salt concentration of $n_s + \Gamma n_e$. This implies that, on the polyelectrolyte solution side, polyions exclude mobile ions from their vicinity and increase the salt concentration of the surrounding solvent domain to $n_s + \Gamma n_e$. Therefore, the test polyion can be regarded as being embedded in a solvent with salt concentration $n_s + \Gamma n_e$, and the effective Debye screening length in the solution with polymer and solvent concentrations n_e and n_s, respectively, may be given by:

$$\kappa^2 = 8\pi Q(n_s + \Gamma n_e) \qquad \text{(A1)}$$

instead of equation (7). For the expression of Γ, we use Manning's theory[25] for polyelectrolyte solutions, that is:

$$\Gamma = (4\xi)^{-1} \qquad \text{(A2)}$$

where ξ is the Manning charge density parameter, which equals 2.1 for xanthan with degree of pyruvation of 0.4. Strictly speaking, the Manning theory is a 'limiting law' that can be applied only to a solution with low ionic strength, so that the use of equation (A2) may lead to some error at higher C_s. However, since it will turn out later that the finite polymer concentration effect on κ does not affect c_i and c_a at high C_s, the error from equation (A2) may not need to be taken as serious.

When a polyelectrolyte solution system separates into an isotropic phase and a liquid-crystal phase, each phase should possess different n_s from the initial salt concentration n_{s0} in the solvent. Thus, in the calculation of c_i and c_a, n_s in equation (A1) must not be equated to n_{s0}. From the equilibrium condition for mobile ions, we obtain:

$$\gamma_{\pm i}^2 n_{si}(n_{si} + n_{ei}) = \gamma_{\pm a}^2 n_{sa}(n_{sa} + n_{ea}) \qquad \text{(A3)}$$

where $\gamma_\pm$ is the mean activity coefficient and the subscripts i and a represent the quantity for the isotropic phase and liquid-crystal phase, respectively. Again from Manning's theory[25], $\gamma_\pm$ is given by:

$$\gamma_\pm^2 = [(X+1)/(\xi X+1)] \exp[X/(X+2)] \qquad \text{(A4)}$$

where $X = \xi^{-1} n_e/n_s$. Substituting equation (A4) into equation (A3), we obtain:

$$n_{ei}^2 (X_i + 1) X_i^{-2} \exp[-X_i/(X_i+2)] = n_{ea}^2 (X_a + 1) X_a^{-2} \exp[-X_a/(X_a+2)] \qquad \text{(A5)}$$

At $c = c_i$, where the amount of the liquid-crystal phase is infinitesimal, n_{si} is equal to n_{s0}, while n_{sa} is calculated from equation (A5) using the given n_{ei} and n_{ea}. On the other hand, at $c = c_a$, where the amount of the isotropic phase is infinitesimal, $n_{sa} = n_{s0}$ and n_{si} is calculated from equation (A5).

Equation (A1) shows that the isotropic and liquid-crystal phases have different κ represented by κ_i and κ_a, respectively, since n_s and n_e are different in the two phases. Taking this difference into account, we calculated the phase boundary concentration c_i using the following iteration method. First, the zero-order approximations to the phase boundary concentrations $c_i(0)$ (or $n_{ei}(0)$) and $c_a(0)$ (or $n_{ea}(0)$) were calculated using both κ_i and κ_a calculated from equation (7) with $n_s=n_{s0}$. In the next step, κ_i and κ_a, which were calculated from equation (A2) with $n_{ei}=n_{ei}(0)$, $n_{ea}=n_{ea}(0)$, $n_{si}=n_{s0}$ and n_{sa} obtained from equation (A5), were used to calculate the first approximations $n_{ei}(1)$ and $n_{ea}(1)$. The same process was iterated until the phase boundary concentrations converged to some values. The convergent value for c_i was taken to be the final c_i. The phase boundary concentration c_a can also be calculated by the same procedure, except for putting $n_{sa}=n_{s0}$, instead of $n_{si}=n_{s0}$ in the above calculation.